Mon. Not. R. Astron. Soc. **330,** L48–L52 (2002)

Can simulations reproduce the observed temperature–mass relation for clusters of galaxies?

Peter A. Thomas,★ Orrarujee Muanwong, Scott T. Kay and Andrew R. Liddle
Astronomy Centre, University of Sussex, Falmer, Brighton BN1 9QJ

Accepted 2002 January 8. Received 2001 December 19

ABSTRACT

It has become increasingly apparent that traditional hydrodynamical simulations of galaxy clusters are unable to reproduce the observed properties of galaxy clusters, in particular overpredicting the mass corresponding to a given cluster temperature. Such overestimation may lead to systematic errors in results using galaxy clusters as cosmological probes, such as constraints on the density perturbation normalization σ_8. In this paper we demonstrate that inclusion of additional gas physics, namely radiative cooling and a possible pre-heating of gas prior to cluster formation, is able to bring the temperature–mass relation in the innermost parts of clusters into good agreement with recent determinations by Allen, Schmidt & Fabian using *Chandra* data.

Key words: hydrodynamics – methods: *N*-body simulations – galaxies: clusters: general – X-rays: galaxies: clusters.

1 INTRODUCTION

Reproducing the observed number density of rich galaxy clusters has long been thought to be one of the most reliable constraints on the matter power spectrum on short scales. It has been studied by many authors over the years (Evrard 1989; Henry & Arnaud 1991; White, Efstathiou & Frenk 1993; Eke, Cole & Frenk 1996; Viana & Liddle 1996, 1999; Henry 1997, 2000; Blanchard et al. 2000; Pierpaoli, Scott & White 2001; Wu 2001), recent determinations typically yielding $\sigma_8 \sim 0.9$ to 1.0 for the currently favoured ΛCDM model with matter density $\Omega_0 \simeq 0.3$. However, recently evidence has begun to accumulate from a number of sources that this may be a significant overestimate, perhaps by tens of per cent. For example, the required σ_8 estimated from the 2dF Galaxy Survey (Lahav et al. 2002; Verde et al. 2002), or from that survey combined with other probes (Efstathiou et al. 2002), is significantly lower, and there are now several papers using galaxy clusters that also give lower results (Borgani et al. 2001; Reiprich & Böhringer 2002; Viana, Nichol & Liddle 2002).

A low value was also found recently by (Seljak 2002), who used an observed relation between cluster temperature and mass (Finoguenov, Reiprich & Böhringer 2001) rather than one derived from hydrodynamical simulations. This last result is particularly significant, and points to the increasingly evident result that traditional hydrodynamical simulations, which include only adiabatic gas heating during collapse, are unable to reproduce the observed properties of clusters. For example, the recent *Chandra* results of Allen, Schmidt & Fabian (2001, hereafter ASF01) indicate that, at least in the inner regions where data exist, clusters are considerably hotter for a given mass than predicted by adiabatic simulations.

Here we address the question of whether the inclusion of additional gas physics, both radiative cooling of the gas and pre-heating of the gas before cluster formation, is capable of bringing the simulations into agreement with observations. We concentrate only on the inner regions of clusters, for which temperature profiles have been measured by *Chandra*, and we find that indeed the observations can be reproduced. In itself this is not sufficient aid to theorists seeking to constrain σ_8, which requires an accurate description of clusters out to the virial radius, but this encouraging result suggests that simulations may soon be useful for this purpose. We will explore the cluster temperature–mass relation out to larger radii in a forthcoming paper.

2 DETERMINING CLUSTER MASSES

2.1 Using the hydrostatic equation to measure masses

The distribution of hot gas in a cluster can be used to measure its mass. The intracluster medium is generally assumed to be in hydrostatic equilibrium in a spherically symmetric, static potential and the mass is determined by balancing pressure support against the gravitational attraction:

$$\frac{1}{\rho_{\rm gas}}\frac{{\rm d}P_{\rm gas}}{{\rm d}r} = -\frac{GM(<r)}{r^2}, \qquad (1)$$

★E-mail: p.a.thomas@sussex.ac.uk

giving

$$M(<r) = \frac{kT_{\rm gas}(r)}{\mu m_{\rm H} G}\left|\frac{{\rm d}\ln P_{\rm gas}}{{\rm d}\ln r}\right| r, \quad (2)$$

where $P_{\rm gas} = (k/\mu m_{\rm H})\rho_{\rm gas}T_{\rm gas}$ is the pressure of the intracluster medium, $\rho_{\rm gas}$ is its density, k is the Boltzmann constant, G is the gravitational constant, and $\mu m_{\rm H} \simeq 1.0\times10^{-24}$ g is the mean mass per particle.

Where $P_{\rm gas}$ is simply the thermal pressure, then $T_{\rm gas}$ corresponds to the gas temperature. One should really include all forms of pressure support for the gas: kinetic (i.e. turbulence), magnetic, coupled relativistic particles, etc. We have checked in our simulations that the contribution from kinetic motions within the inner regions of clusters is small and so for clarity of presentation we stick with the thermal pressure in this paper.

Note that the determination of the mass within radius r depends only upon the properties of the gas at that radius; in particular the mass determination is not affected by conditions in the outer parts of clusters where the properties are poorly determined. We show in Section 4.1 that the use of equation (2) leads to good estimates of the mass within regions accessible to *Chandra* observations. This lends credence to the mass determinations from X-ray observations that we use in this paper.

2.2 Observed and simulated temperature–mass relations

If we apply equation (2) to measure the mass, M_Δ, within a radius, r_Δ, for which the enclosed density is Δ times the critical density, then

$$\frac{kT(r_\Delta)}{\rm keV} \approx 8.3\left(\frac{\Delta}{200}\right)^{1/3}\left(\frac{\mathcal{P}_\Delta}{2}\right)^{-1}\left(\frac{M_\Delta}{10^{15}h^{-1}\,{\rm M}_\odot}\right)^{2/3}, \quad (3)$$

where $\mathcal{P}_\Delta = -{\rm d}\ln P_{\rm gas}/{\rm d}\ln r$ measured at r_Δ.

For self-similar clusters, for which $\mathcal{P}_\Delta$ is independent of mass and $T(r_\Delta)$ is a constant multiple of the observed temperature, $T_{\rm X}$, we recover a scaling relation $T_{\rm X} \propto M_\Delta^{2/3}$. In order to compare different results we will write

$$\frac{kT_{\rm X}}{\rm keV} = A_\Delta\left(\frac{M_\Delta}{10^{15}h^{-1}\,{\rm M}_\odot}\right)^{\alpha}. \quad (4)$$

A_Δ gives the relative normalization of the relations; if $\alpha \neq 2/3$ then this comparison will be exact only for $M_\Delta = 10^{15}\,h^{-1}\,{\rm M}_\odot$. Theorists can most easily predict the mass within the virial radius of a cluster, corresponding to $\Delta \simeq 111$ for our chosen cosmology, but X-ray observations do not extend to such large radii and so some degree of extrapolation (i.e. the extension of a mass-model beyond the range of the observational data) is usually required.

A useful summary of simulated and observational results is given by Afshordi & Cen (2002). The main simulated catalogues are by Evrard, Metzler & Navarro (1996), Thomas et al. (2001) and Bryan & Norman (1998). The former two, using smoothed particle hydrodynamics (SPH), found $A_{200} \approx 8.0$, whereas the latter, using an Eulerian grid-code, found $A_{200} \approx 7.0$. In a more recent paper, in which they considered a variety of definitions of X-ray temperature for an ensemble of 24 highly resolved SPH clusters, Mathiesen & Evrard (2001) agreed with this lower normalization. None of these simulations included radiative cooling.

By contrast the observational results using resolved surface brightness and temperature profiles from *ROSAT* and *ASCA* have higher normalizations. Xu, Jin & Wu (2001) find $A_{200} \approx 9.4$, whereas Horner, Mushotzky & Scharf (1999) and Finoguenov et al. (2001) both find $A_{200} \approx 11.2$.

Despite the uncertainty in both the simulated and the observational results, it is clear that the observed normalization of the temperature–mass relation significantly exceeds the simulated one.

2.3 Observational determination of M_{2500}

In this paper, we attempt a partial resolution of the differences between simulations and observations discussed in the previous section. In doing this, we concentrate on the results of ASF01. The reasons for this are fourfold.

(i) *Chandra* observations give the best available estimates of density and temperature profiles for the X-ray-emitting gas.

(ii) The mass estimates are, mostly, backed up by observations and modelling of gravitationally lensed background galaxies (arcs).

(iii) They present results for the mass-weighted temperature of the gas. The use of mass-weighted rather than emission-weighted temperatures greatly simplifies the comparison of simulations and observations.

(iv) They do not attempt to extrapolate their results beyond the radius that is accessible to observations.

ASF01 measured the mass and temperature of five clusters within r_{2500}. They found a best-fitting slope for the mass–temperature relation that is consistent with the self-similar value of 1.5. We rewrite their relation here with mass as the ordinate as we are complete in mass rather than temperature in our simulations:

$$\frac{kT_{2500}}{\rm keV} \approx 19.2\left(\frac{M_{2500}}{10^{15}h^{-1}\,{\rm M}_\odot}\right)^{2/3}, \quad (5)$$

where T_{2500} is the mass-weighted gas temperature within r_{2500}.

3 SIMULATIONS

The simulations that we discuss in this paper were carried out using the HYDRA *N*-body/hydrodynamics code (Couchman, Thomas & Pearce 1995; Pearce & Couchman 1997) on the Cray T3E computer at the Edinburgh Parallel Computing Centre as part of the Virgo Consortium programme of investigations into structure formation in the Universe. They will be described fully in a longer paper (in preparation) and so we just summarize the properties here. Note that the simulations are very similar to those discussed in an earlier paper (Muanwong et al. 2001), but the parameters have been slightly adjusted so as to give a better fit to the observed luminosity–temperature relation of clusters.

In this paper we present results for a single cosmology with density parameter $\Omega_0 = 0.35$, cosmological constant $\Omega_{\Lambda 0} = 0.65$, baryon density $\Omega_{\rm b0} = 0.038$, Hubble parameter $h = 0.71$, cold dark matter (CDM) density fluctuation parameter $\Gamma = 0.21$, normalization $\sigma_8 = 0.90$ and gravitational softening $s = 25\,h^{-1}$ kpc. 160^3 particles each of gas and dark matter were used in a box of side $100\,h^{-1}$ Mpc, giving particle masses of $m_{\rm gas} \approx 2.6\times10^9\,h^{-1}\,{\rm M}_\odot$ and $m_{\rm dark} \approx 2.1\times10^{10}\,h^{-1}\,{\rm M}_\odot$, respectively.

Three simulations were undertaken, each with identical initial conditions so that the clusters that they produce are directly comparable, but with different cooling properties.

(i) *Non-radiative.* An adiabatic run included for testing and

comparison purposes only. As discussed by Muanwong et al. (2001), the gas in the centres of the clusters extracted from this run has short cooling times and would not be present in real systems. This simulation vastly overestimates the X-ray luminosity of the clusters.

(ii) *Radiative.* This run includes radiative cooling using the cooling tables of Sutherland & Dopita (1993) and assumes a time-varying metallicity $Z = 0.3(t/t_0)\,Z_\odot$, where t/t_0 is the age of the Universe in units of the current time. Cooled material is permitted to form stars, removing low-entropy material with short cooling times from the centres of the clusters. As shown by Pearce et al. (2000), the inflowing gas which replaces it has a higher net entropy and hence a higher temperature. A drawback of this run is that the cooling is limited only by numerical resolution and is therefore very ad hoc. In this run up to half the baryonic mass in clusters has cooled, much more than is observed.

(iii) *Pre-heating.* This run also includes radiative cooling. Additionally, at $z = 4$ the energy of each gas particle was increased by an amount $kT = 1\,\mathrm{keV}$ to model crudely energy injection at high redshift. This has the effect of strongly suppressing cooling so that by the end of the simulation under 1 per cent of the gas in clusters has cooled, much less than is observed.

The radiative and pre-heating runs both reproduce the observed luminosity–temperature relation whilst having very different amounts of cooled gas. One might hope, therefore, that their thermal properties also bracket those of real clusters. We justify this statement further in Section 4.3 below.

4 RESULTS

4.1 Hydrostatic equilibrium

Fig. 1 compares measures of enclosed mass versus radius for the third-largest cluster in the pre-heating simulation (similar results are obtained for the non-radiative and radiative simulations). This particular cluster was chosen because the two largest clusters both show signs of disturbance within r_{500}. The solid line shows enclosed mass as a function of radius. The dashed line shows the mass estimated from equation (2) using the thermal pressure; a similar result is obtained using the total (thermal plus kinetic) pressure but we have omitted this from the plot for clarity.

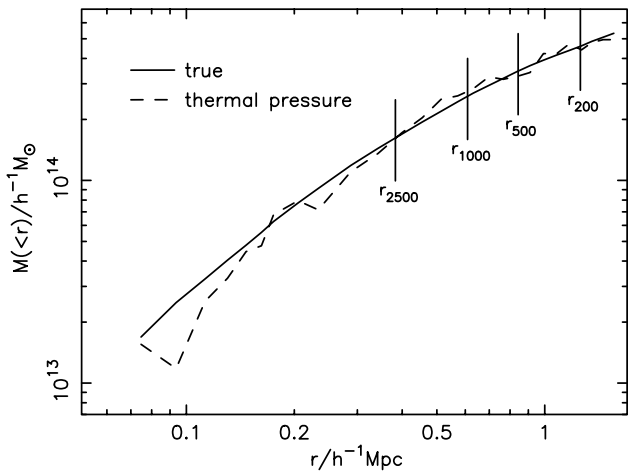

Figure 1. The solid line shows the actual mass distribution in the cluster; the dashed line shows the mass from equation (2) using the thermal pressure.

The estimated mass jiggles up and down because of variations in the local pressure gradient. This scatter could be much reduced by the fitting of a smooth curve to the pressure profile, but for the purposes of this paper we merely wish to make the point that the clusters are in approximate hydrostatic equilibrium within r_{2500}. This holds true also for the largest two clusters and for all others that we have tested. Note, however, that many of these other clusters show significant departures from equilibrium within r_{200}.

We conclude that the use of the equation of hydrostatic support to measure masses from X-ray observations of the intracluster medium within r_{2500} is likely to be accurate to within about 10 per cent with no systematic offset to high or low masses.

4.2 Temperature profiles

Fig. 2 shows the projected temperature profiles within r_{2500} of the third-largest cluster in each of the three simulations. Note how the inflow of higher entropy material has raised the temperature of the gas within r_{2500} in both the radiative and pre-heating simulations relative to that in the non-radiative simulation, an effect first noted by Pearce et al. (2000). The temperature profiles in this figure differ from those shown in fig. 1 of ASF01 in that they decline slightly beyond $0.25\,r_{2500}$ rather than remaining isothermal. There are other clusters in our sample, however, for which the temperature profiles are very similar to those seen in the observations.

4.3 Entropy profiles

The differences between the three simulations are best described in terms of their entropy profiles. As Fig. 3 shows, the entropy within r_{1000} in the third-largest cluster is raised in the radiative and pre-heating runs relative to that in the non-radiative run. This results in a higher gas temperature and a less-peaked density profile.

Although the radiative and pre-heating runs have very different cooled mass fractions, it is not surprising that they have similar entropy profiles as we have adjusted the numerical resolution and feedback parameters so as to reproduce the observed X-ray luminosity–temperature relation, and it has been recognized for some time that this requires an excess of entropy in cluster cores (Evrard & Henry 1991; Kaiser 1991; Bower 1997). Once the entropy profile is fixed then, assuming hydrostatic equilibrium, the

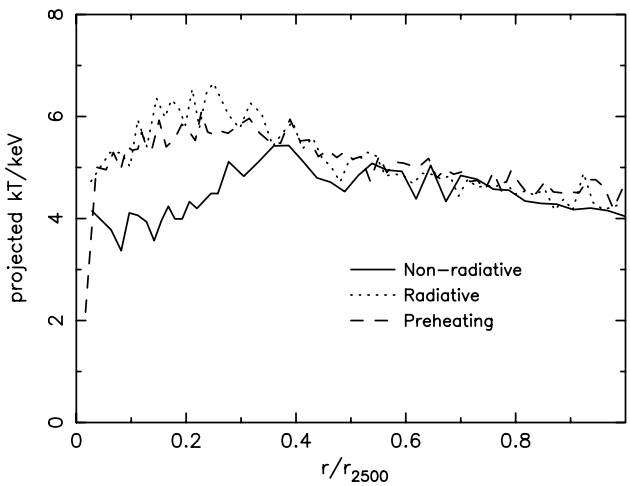

Figure 2. Temperature profile of the gas within r_{2500} for one example cluster in the three simulations.

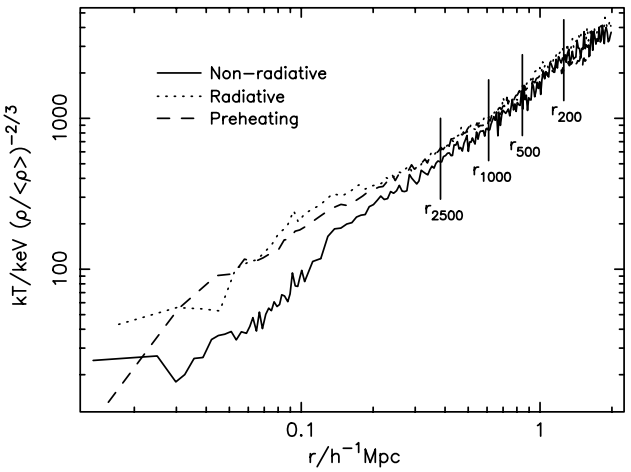

Figure 3. Entropy profile of the gas for one example cluster in each of the three simulations.

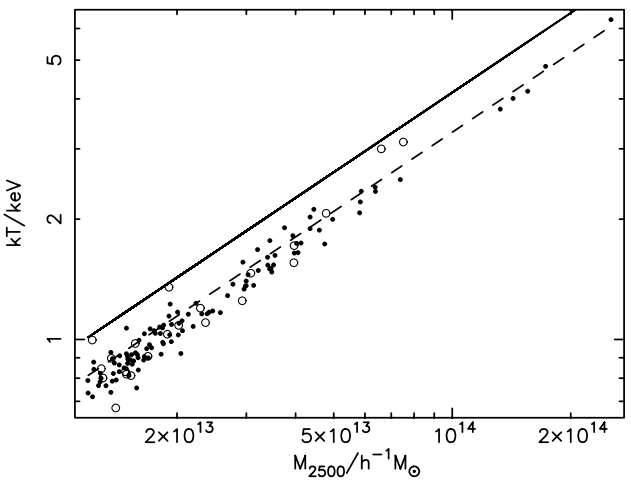

Figure 4. The mass-weighted temperature–mass relation for gas within r_{2500} for clusters extracted from the non-radiative simulation. Different symbols correspond to clusters with different amounts of substructure, as discussed in the text. The solid line shows the best fit from ASF01; the dashed line shows (extrapolated) results from the simulations of Mathiesen & Evrard (2001).

cluster temperature profile is uniquely determined. As it happens, both the radiative and pre-heating runs give very similar entropy profiles and hence very similar temperature profiles for this cluster (and similar results are obtained for other clusters). This gives us confidence that other models that reproduce the luminosity–temperature relation, and in particular ones that give the correct cooled gas fraction, would have similar thermal properties to those discussed here.

4.4 Temperature–mass relation

The temperature–mass relation for the clusters extracted from the non-radiative simulation is shown in Fig. 4. The dashed line is the relation from the simulations of Mathiesen & Evrard (2001), extrapolated from their results for an overdensity of 500 as described in ASF01. Given this extrapolation our results are in good agreement with theirs over the range for which our temperatures coincide, $kT \gtrsim 1.5$ keV. By contrast, the relation for observed clusters obtained in ASF01, shown by the solid line, has a significantly lower mass normalization for a given temperature.

Fig. 5 shows how this relation is modified once extra gas physics is incorporated. We see that the increase in temperature associated with radiative cooling and/or pre-heating is precisely enough to bring the simulated relation into agreement with the observed one.

In the figures there are several clusters that lie well above the mean relation. These are mostly clusters for which there is significant velocity substructure; we indicate with open circles those clusters for which the mean gas and dark matter velocities within r_{2500} differ by more than 10 per cent of the rms velocity dispersion of the dark matter.

5 DISCUSSION

We have shown that simulations are capable of reproducing the observed relationship between mass and temperature in the inner regions of galaxy clusters. In particular, the mass-weighted temperature versus mass within a radius enclosing an overdensity of 2500 in our radiative and pre-heating simulations agrees with the observed relation of ASF01.

There are a number of caveats, however. The temperature ranges of the simulations and the observations barely overlap: we have one cluster above 6 keV, while ASF01 have only one below this

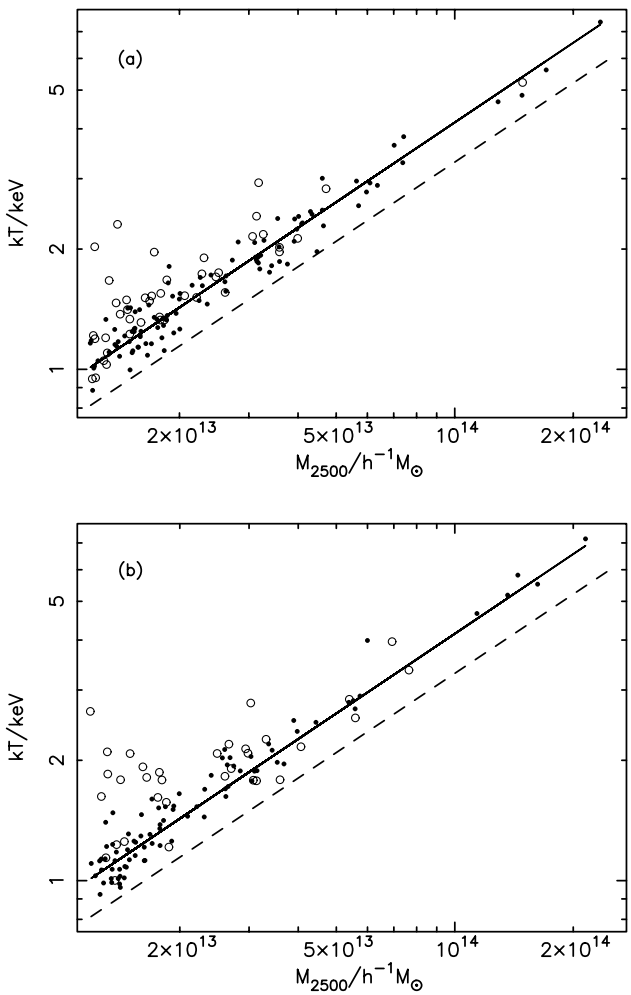

Figure 5. As Fig. 4, but for the (a) radiative and (b) pre-heating simulations.

temperature. Nevertheless, there is no reason to suppose that our results will not extend up to higher temperatures, although confirmation of this will have to await re-simulations of clusters drawn from larger simulation boxes.

Perhaps more pertinently, none of our simulations presents a fully realistic model of clusters, the radiative model producing too much cooled gas and the pre-heating model too little. However, they both match the observed X-ray luminosity–temperature relation, because they both have a higher entropy within r_{2500} than does the non-radiative simulation. This increase in entropy manifests itself as an increase in the temperature of the gas in the inner parts of the clusters. One might expect, therefore, that realistic clusters that share the same entropy profile would predict the same temperature–mass relation.

Unfortunately, the results presented in this paper and in ASF01 are of limited use to theorists who wish to predict the temperature function of clusters in order to constrain cosmology. This is because they need to relate the mass within the virial radius to the emission-weighted temperature of clusters. The prediction of masses at r_{500} or larger radii from the X-ray observations is a harder problem than discussed here and will be investigated in a longer paper.

ACKNOWLEDGMENTS

The simulations used in this paper were carried out on the Cray-T3E at the EPCC as part of the Virgo Consortium programme of investigations into the formation of structure in the Universe. PAT is a PPARC Lecturer Fellow; OM is supported by a DPST scholarship from the Thai government, STK by PPARC, and ARL in part by the Leverhulme Trust.

REFERENCES

Afshordi N., Cen R., 2002, ApJ, in press (astro-ph/0105020)
Allen S. W., Schmidt R. S., Fabian A. C., 2001, MNRAS, 328, L37 (ASF01)
Blanchard A., Sadat R., Bartlett J. G., le Dour M., 2000, A&A, 362, 809
Borgani S. et al., 2001, ApJ, 561, 13
Bower R. G., 1997, MNRAS, 288, 355
Bryan G. L., Norman M. L., 1998, ApJ, 495, 80
Couchman H. M. P., Thomas P. A., Pearce F. R., 1995, MNRAS, 452, 797
Efstathiou G. et al., (the 2dF team), 2002, MNRAS, submitted (astro-ph/0109152)
Eke V. R., Cole S., Frenk C. S., 1996, MNRAS, 282, 263
Evrard A. E., 1989, ApJ, 341, L71
Evrard A. E., Henry J. P., 1991, ApJ, 383, 95
Evrard A. E., Metzler C. A., Navarro J. F., 1996, ApJ, 469, 494
Finoguenov A., Reiprich T. H., Böhringer H., 2001, A&A, 368, 749
Henry J. P., 1997, ApJ, 489, L1
Henry J. P., 2000, ApJ, 534, 565
Henry J. P., Arnaud K. A., 1991, ApJ, 372, 410
Horner D. J., Mushotzky R. F., Scharf C. A., 1999, ApJ, 520, 78
Kaiser N., 1991, ApJ, 383, 104
Lahav O. et al., (the 2dF team), 2002, MNRAS, submitted (astro-ph/0112162)
Mathiesen B. F., Evrard A. E., 2001, ApJ, 546, 100
Muanwong O., Thomas P. A., Kay S. T., Pearce F. R., Couchman H. M. P., 2001, ApJ, 552, L27
Pearce F. R., Couchman H. M. P., 1997, New Astron., 2, 411
Pearce F. R., Thomas P. A., Couchman H. M. P., Edge A. C., 2000, MNRAS, 317, 1029
Pierpaoli E., Scott D., White M., 2001, MNRAS, 325, 77
Reiprich T. H., Böhringer H., 2002, ApJ, in press (astro-ph/0111285)
Seljak U., 2002, MNRAS, submitted (astro-ph/0111362)
Sutherland R. S., Dopita M. A., 1993, ApJS, 88, 253
Thomas P. A., Muanwong O., Pearce F. R., Couchman H. M. P., Edge A. C., Jenkins A., Onuora L., (the Virgo Consortium), 2001, MNRAS, 324, 450
Verde L. et al., (the 2dF team), 2002, MNRAS, submitted (astro-ph/0112161),
Viana P. T. P., Liddle A. R., 1996, MNRAS, 281, 323
Viana P. T. P., Liddle A. R., 1999, MNRAS, 303, 535
Viana P. T. P., Nichol R. C., Liddle A. R., 2002, ApJ, submitted (astro-ph/0111394)
White S. D. M., Efstathiou G., Frenk C. S., 1993, MNRAS, 262, 1023
Wu J.-H. P., 2001, MNRAS, 327, 629
Xu H., Jin G., Wu X.-P., 2001, ApJ, 553, 78

This paper has been typeset from a TEX/LATEX file prepared by the author.